Research paper

Effects of short-term food deprivation on catecholamine and metabolic-sensory biomarker gene expression in hindbrain A2 noradrenergic neurons projecting to the forebrain rostral preoptic area: Impact of negative versus positive estradiol feedback

Ayed A. Alshamrani, Mostafa M.H. Ibrahim, Karen P. Briski[*]

School of Basic Pharmaceutical and Toxicological Sciences, College of Pharmacy, University of Louisiana at Monroe, Monroe, LA 71201, USA

ABSTRACT

Hindbrain A2 noradrenergic neurons assimilate estrogenic and metabolic cues. In female mammals, negative-versus positive-feedback patterns of estradiol (E) secretion impose divergent regulation of the gonadotropin-releasing hormone (GnRH)-pituitary-gonadal (HPG) neuroendocrine axis. Current research used retrograde tracing, dual-label immunocytochemistry, single-cell laser-microdissection, and multiplex qPCR methods to address the premise that E feedback modes uniquely affect metabolic regulation of A2 neurons involved in HPG control. Ovariectomized female rats were given E replacement to replicate plasma hormone levels characteristic of positive (high-E dose) or negative (low-E dose) feedback. Animals were either full-fed (FF) or subjected to short-term, e.g., 18-h food deprivation (FD). After FF or FD, rostral preoptic area (rPO)-projecting A2 neurons were characterized by the presence or absence of nuclear glucokinase regulatory protein (nGKRP) immuno-staining. FD augmented or suppressed mRNAs encoding the catecholamine enzyme dopamine-beta-hydroxylase (DβH) and the metabolic-sensory biomarker glucokinase (GCK), relative to FF controls, in nGKRP-immunoreactive (ir)-positive A2 neurons from low-E or high-E animals, respectively. Yet, these transcript profiles were unaffected by FD in nGKRP-ir-negative A2 neurons at either E dosage level. FD altered estrogen receptor (ER)-alpha and ATP-sensitive potassium channel subunit sulfonylurea receptor-1 gene expression in nGKRP-ir-positive neurons from low-E, but not high-E animals. Results provide novel evidence that distinct hindbrain A2 neuron populations exhibit altered versus unaffected transmission to the rPO during FD-associated metabolic imbalance, and that the direction of change in this noradrenergic input is controlled by E feedback mode. These A2 cell types are correspondingly distinguished by FD-sensitive or -insensitive GCK, which correlates with the presence versus absence of nGKRP-ir. Further studies are needed to determine how E signal volume regulates neurotransmitter and metabolic sensor responses to FD in GKRP-expressing A2 neurons.

1. Introduction

Metabolic status is tightly coupled with neural regulation of reproduction in female mammals. Negative energy balance impairs fecundity in women and in food and laboratory animals. As female reproduction (encompassing ovulation, conception, pregnancy, and lactation) requires significant energy investment, impedance or suspension of this complex process by metabolic instability prevents energy waste (Wade and Jones, 2004). Dedicated metabolic-sensory neurons in the hindbrain dorsal vagal complex (DVC) provide a dynamic readout of cellular energy state (Oomura and Yoshimatsu, 1984). The hindbrain is the principal source of metabolic deficit cues that restrain pituitary luteinizing

hormone (LH) secretion (Ohkura et al., 2000). Evidence that intra-hindbrain glucose anti-metabolite drug administration inhibits rostral preoptic area (rPO) gonadotropin-releasing hormone (GnRH) neuron transcriptional activation and suppresses LH secretion in female rats confirms hindbrain metabolic sensor control of the GnRH-pituitary gonadotropin neuroendocrine axis in this sex (Singh and Briski, 2004; Ibrahim and Briski, 2014). Caudal DVC A2 noradrenergic neurons are a plausible source of hindbrain metabolic input to the reproductive neuroendocrine axis as the catecholamine transmitter norepinephrine (NE) has a well-characterized role in GnRH-LH regulation (Demling et al., 1985; Mohankumar et al., 1994; Szawka et al., 2013), and these cells express molecular biomarkers for metabolic-sensory function, i.e. glucokinase (GCK), ATP-sensitive potassium channels (K_{ATP}), and the ultra-sensitive energy sensor, adenosine 5′-monophosphate-activated protein kinase (AMPK) (Briski et al., 2009; Cherian and Briski, 2011; Ibrahim et al., 2013).

Estradiol (E) acts on the female brain to impose tonic inhibition and phasic, i.e. cyclic stimulation of the GnRH-LH axis by negative- versus positive-feedback mechanisms, respectively. This hormone also regulates systemic energy balance through control of energy intake, storage, and expenditure. E secretion varies substantially over the female rat estrous cycle, as nadir (negative feedback mode) versus peak (positive feedback mode) plasma hormone concentrations vary by more than 4–5 fold (Butcher et al., 1974; Goodman, 1978). Negative- and positive-feedback modes of E output exert disparate effects on systemic metabolic stability as food intake declines and energy state becomes ironically more negative as circulating E levels rise (Giles et al., 2010). Maintenance of energy homeostasis despite variable environmental nutrient provision and dynamic adjustments in internal energy needs poses a constant challenge. The ideal circumstance of unfettered ability to eat-at-will in response to the interplay of these complex processes can be impractical in reality. Indeed, short-term suspension of food intake, planned or unplanned, is an unavoidable and unpredictable metabolic stressor inherent to modern life. E controls physiological responses to metabolic imbalance due to interrupted feeding, as short-term food deprivation (FD) elicits E-dependent hyperphagia and plasma substrate fuel and energy deficit-sensitive hormone profiles in ovariectomized (OVX) female rats (Ibrahim and Briski, 2015; Alenazi et al., 2016; Briski et al., 2016). Our studies also show that FD suppresses the GnRH-LH axis by hindbrain metabolic sensor-dependent mechanisms in the presence of positive-, but not negative feedback levels of E (Shakya et al., 2018). E evidently acts in part to regulate hindbrain metabolic sensing of cellular instability as this hormone controls DVC GCK and SUR-1 transcriptional reactivity to hypoglycemia (Vavaiya and Briski, 2008).

A2 neurons express estrogen receptor (ER)-alpha (ERα) and -beta (ERβ) mRNAs and proteins (Ibrahim et al., 2013; Tamrakar et al., 2015), and mediate estradiol feedback control of reproductive neuroendocrine function (Ibrahim and Briski, 2014). Bimodal E regulation of reproductive neuroendocrine function is achieved, in part, by E concentration-dependent patterns of NE input to the forebrain preoptic area (Wise et al., 1981; Adler et al., 1983; Demling et al., 1985). Metabolic-sensitive GnRH neurons reside in the rPO (Briski and Sylvester, 1998). Current research used a validated *in vivo* E replacement paradigm that establishes plasma hormone levels at estrous cycle nadir versus peak concentrations (Goodman, 1978; Briski et al., 2001) to determine if A2 neurons that innervate the rPO are direct substrates for both estrogenic and metabolic inputs, and to address the premise that negative- versus positive-feedback patterns of E secretion control how FD may regulate A2 noradrenergic transmission to the rPO. Here, fluorescent retrograde neuronal labeling, dual-label immunocytochemistry, single-cell laser-microdissection, and single-cell multiplex qPCR techniques were employed to analyze FD effects on catecholamine enzyme (dopamine-beta-hydroxylase; DβH), metabolic sensor [GCK; K_{ATP} sulfonylurea receptor-1 (SUR-1) subunit], and ERα and ERβ gene expression in rPO-projecting A2 neurons collected from OVX rats treated with E to mimic estrous cycle nadir versus peak plasma E concentrations.

Glucokinase regulatory protein (GKRP) regulates GCK enzyme activity and subcellular localization through formation of GKRP-GCK complexes (Agius, 2008; Agius, 2016; Sternisha and Miller, 2019). Glucose and GKRP compete for binding to GCK; GKRP-GCK complexes are formed when cellular glucose levels wane, causing deactivation of GCK, and then translocate to the nucleus. Our working premise here was that the presence versus absence of nuclear GKRP immunostaining of rPO-projecting A2 neurons would differentiate these cells into subtypes that (1) express GCK and engage in metabolic-sensory function or (2) lack GCK.

2. Materials and (ethods

2.1. Animals

Adult female Sprague Dawley rats (250–300 g *bw*) were housed 2–3 per cage under a 14 hr light/10 h dark cycle (lights on at 05.00 h), and allowed free access to standard laboratory chow diet (Harlan Teklad LM-485; Harlan industries, Madison, WI) and tap water. All surgical and experimental protocols were conducted in accordance with The NIH Guide for the Care and Use of Laboratory Animals, 8th Edition, under approval by the ULM Institutional Animal Care and Use Committee. Animals were gentled on a daily basis to facilitate acclimation to handling.

2.2. Experimental design

Animals: On Study Day 1, rats were injected subcutaneously (*sc*) with ketamine/xylazine (0.1 mL/100 g *bw*; 90 mg ketamine: 10 mg xylazine/mL; Covetrus, Portland, ME) prior to bilateral ovariectomy (OVX) and bilateral stereotactic injection of Retrobead retrograde tracer (1.0 μL, infused at a rate of 3.6 μL/min; Lumafluor Corp., Durham, NC) into the rostral preoptic area (rPO) at pre-determined coordinates [anterior-posterior: 0 mm from *bregma*; lateral: ± 0.2 mm lateral to midline; dorsal-ventral: 6.8 mm ventral to skull surface] using a Hamilton 1701 gastight syringe aided by a stereotaxic Drill Injection Robot (Neurostar, Tubingen, Germany) [Uddin et al., 2021]. This system features atlas integration, intuitive computer control of the stereotaxic frame, sensor detection of brain surface, and alignment correction for fully-automated drill/injection robot-performed depth-controlled drilling and needle placement. Prior work from our laboratory involved stereotaxic delivery of pharmacological compounds into several discrete preoptic structures, including the rPO (Ibrahim and Briski, 2014). At the conclusion of surgery, animals were injected with ketoprofen *sc* and enrofloxacin IM and treated by topical administration of 0.25 % bupivacaine to closed incisions prior to transferral to individual cages. On Study Day 7, animals were anesthetized with isoflurane (5 % - induction; 2.5 % - maintenance), then implanted *sc* with a silastic capsule (10 mm/100 g *bw*; 0.062 in. *i.d.*/0.125 in. *o.d.*) filled with 17β-estradiol-3-benzoate at a concentration of 30 (E-30) or 300 (E-300) μg/mL safflower oil, as described (Briski et al., 2001). These estradiol dosages yield circulating hormone levels that mimic plasma E levels measured on metestrus or proestrus, respectively, in ovary-intact adult cycling female rats (Butcher et al., 1974). Groups of E-30 and E-300 rats were randomly divided into the following treatment groups: (1) full-fed (FF; n = 5 E-30; n = 5 E-300); (2) food-deprived (FD; initiated at 21.00 h on day 10; n = 5 E-30; n = 5 E-300). Animals were sacrificed at 16.00 h on day 11 for brain and trunk blood collection. Accuracy of bilateral needle placement into the rPO was confirmed by visual examination of consecutive frozen tissue sections containing the rPO during the process of cutting those sections for subsequent rPO micropunch dissection for Western blot analysis of GnRH-1 protein expression.

Hindbrain A2 Noradrenergic Neuron Laser-Catapult Microdissection: Serial 10 μm-thick frozen tissue sections were cut from each hindbrain between − 14.36 and − 14.86 mm posterior to *bregma* and mounted on polyethylene naphthalate membrane-covered slides (Carl Zeiss

MicroImaging, White Plains, NY) for epifluorescence visualization of cytoplasmic retrograde tracer and dual-label immunohistochemical staining for cytoplasmic tyrosine hydroxylase (TH)-immunoreactivity (-ir) and nuclear glucokinase regulatory protein (GCKR)-ir. Briefly, a 1 in 3 series of sections were washed with 0.05 M Tris-buffered saline (TBS, pH 7.6), pre-incubated with 4.0 % normal donkey serum (prod. no. S30; EMD Millipore, Billerica, MA), then incubated for 48 hr at 4 °C with a mouse monoclonal antiserum against TH (prod. no. 22941, 1:600; Immunostar, Hudson, WI) diluted in TBS containing 0.05 % Triton X-100. Sections were then incubated overnight with AlexaFluor-488 donkey anti-mouse IgG secondary antibody (prod. no. 715–545–151, 1:400; Jackson ImmunoResearch Laboratories, Inc., West Grove, PA) diluted in TBS containing 2.0% normal donkey serum. Next, tissues were incubated for 10 min with Endogenous HRP/AP Blocking Solution (prod. no. SP-6000, Vector Laboratories, Inc., Burlingame, CA), followed by incubation for 72 h at 4 °C with a rabbit polyclonal anti-GKRP antiserum (prod. no. NBP2–1662, 1:500; Novus Biologicals, LLC, Littleton, CO). After incubation for 2 hr with peroxidase-labeled donkey anti-rabbit IgG antibody (prod. No. 711–035–152, 1:200; Jackson ImmunoRes.), tissues were processed with ImmPACT DAB peroxidase Substrate kit reagents (prod. no. SK-4103, Vector Lab.). A P.A.L.M. UV-A Microlaser IV System (Carl Zeiss MicroImaging) was utilized to isolate and collect single neurons from the A2 cell area exhibiting the following characteristics: (1) cytoplasmic red retrograde tracer epifluorescence-positive, cytoplasmic TH-immunoreactivity (-ir)-positive, nuclear GKRP-ir-positive, or (2) cytoplasmic red retrograde tracer epifluorescence-positive, cytoplasmic TH-ir-positive, nuclear GKRP-ir-negative. Individual microdissected neurons were each collected into a separate adhesive cap (prod. no. 415190–9181–000; Carl Zeiss Micro-Imaging) for qPCR gene expression analysis by methods established in our laboratory (Vavaiya and Briski, 2008; Briski et al., 2009; Genabai et al., 2009; Cherian and Briski, 2011). A cell collection strategy outlined in earlier work (Briski et al., 2009) was implemented here, wherein two TH-ir-/epifluorescence-positive A2 neurons were acquired from each animal per treatment group; one was nuclear GKRP-ir-positive, while the other was GKRP-ir-negative. Sample numbers utilized here allowed successful performance of appropriate ANOVA and *post-hoc* statistical analyses.

Single-cell multiplex quantitative real-time PCR analysis: *cDNA Synthesis and Amplification*: *Complementary DNA (cDNA) Synthesis and Amplification:* Individual cell lysates were obtained by centrifugation (3000 rpm; 4°C), then incubated at 25 °C (10 min) and at 75 °C (5 min) in an iQ™5 iCycler (Bio-Rad, Hercules, CA) to remove genomic DNA. Sample RNA integrity, purity, and quantity was determined in a Bio-Rad Experion gel-based electrophoresis system, as described [Vavaiya and Briski (Vavaiya and Briski, 2008)]. RNA was reverse-transcribed to cDNA by addition of 1.5 μL cDNA synthesis buffer (iScript™ Advanced cDNA Synthesis Kit; prod. no. 1725038; Bio-Rad), followed by sequential incubation at 46 °C (20 min) and 95 °C (1 min). A preamplification master mix was created by pooling PrimePCR™ PreAmp for SYBR® Green Assays for DβH (prod. no. qRnoCED0002996; Bio-Rad), GCK (prod. no. qRnoCID0009394; Bio-Rad), SUR-1 (prod. no. qRnoCED0001490; Bio-Rad), ERα (prod. no. qRnoCID0009588; Bio-Rad), ERβ (prod. no. qRnoCID0008785; Bio-Rad), and GAPDH (prod. no. qRnoCID0057018; Bio-Rad) with SsoAdvanced™ PreAmp Supermix (prod. no. 1725160; Bio-Rad). Preamplification of cDNA was done by addition of 9.5 μL preamplification master mix to each cDNA sample before thermal cycler incubation at 95 °C (3 min), followed by 10 cycles of incubation at 95 °C (15 s), then 60 °C (4 min). Preamplified cDNA samples were diluted by addition of 185 μL IDTE (prod. no. 11–05–01–05; 1X TE solution; Integrated DNA Technologies, Inc., Coralville, IA). *qPCR Analysis*: PCR samples were prepared by combining primers [DβH (0.5 μL; prod. no. qRnoCED0002996; Bio-Rad), GCK (0.5 μL; prod. no. qRnoCID0009394; Bio-Rad), SUR-1 (0.5 μL; prod. no. qRnoCED0001490; Bio-Rad), ERα (0.5 μL; prod. no. qRnoCID0009588; Bio-Rad), ERβ (0.5 μL; prod. no. qRnoCID0008785; Bio-Rad), and

GAPDH (0.5 μL; prod. no. qRnoCID0057018; Bio-Rad)], cDNA sample (2 μL), and iTaq™ Universal SYBR® Green Supermix (5 μL, prod. no. 1725121; Bio-Rad). Samples were added to individual wells of hard-shell 384-well PCR plates (prod. no. HSP3805, Bio-Rad) for analysis in a Bio-Rad CFX384™ Touch Real-Time PCR Detection System by initial denaturation at 95 °C (30 s), followed by 40 cycles of 3 s incubation at 95 °C and 30 s incubation at 59 °C for DβH, 58.8 °C for GCK, 59.1 °C for SUR1, 58 °C for ERα, 59.2 °C for ERβ, or 57.3 °C for GAPDH, respectively. Melt curve analyses were performed to identify non-specific products and primer dimers. Data were analyzed by the $2^{\Delta\Delta Ct}$ or comparative Ct method and expressed relative to the reference gene GAPDH [Livak and Schmittgen, 2001].

Micropunch-Dissection and Western Blot Analysis of rPO Tissue: Calibrated hollow needles (0.5 mm diameter; prod. no. 57401, Stoelting Co., Wood Dale, IL), were used to bilaterally dissect the rPO from 100 μm-thick frozen sections cut from +0.2–0.00 mm relative to *bregma*, as described (Shakya et al., 2018). For each animal, micropunch tissue samples were pooled by collection into Western blot lysis buffer, e.g., 2.0 % SDS, 0.05 M DTT, 10.0% glycerol, 1.0 mM EDTA, 60 mM Tris-HCl, pH 7.2, and heat-denatured. For each treatment group, aliquots from individual subjects were pooled to create three separate sample pools for GnRH-1 immunoblotting. Proteins were separated in Stain-Free TGX 10% gels, as reported [Ibrahim et al., 2019]; after electrophoresis, gels were activated for 1 min by UV light in a Bio-Rad ChemiDoc™ Touch Imaging System prior to protein transfer to 0.45-μm PVDF-plus membranes (prod. no. 1212639; Data Support Co., Panorama City, CA). Membrane buffer washes and antibody incubations were performed by Freedom Rocker™ Blotbot® automation (Next Advance, Inc., Troy NY). After blocking (2 h) with Tris-buffered saline (TBS), pH 7.4, containing 0.2 % Tween-20 (prod. no. 9005–64–5; VWR, Radnor, PA) and 2% bovine serum albumin (BSA) (prod. no. 9048–46–8; VWR), membranes were probed (48 h; 4 °C) for GnRH-1 by incubation with a mouse GnRH-1 primary antibody [prod. no. sc-32292, 1:1000; Santa Cruz Biotechnology, Inc,. Santa Cruz, CA], then incubated (1 hr) with a horseradish peroxidase-labeled goat anti-rabbit IgG secondary antiserum (prod. no. NEF812001EA, PerkinElmer, Boston, MA; 1:5000), followed by exposure to SuperSignal West Femto maximum-sensitivity chemiluminescent substrate (prod. no. 34096, ThermoFisherScientific, Waltham, MA). Target protein optical density (O.D.) signals were visualized in the ChemiDoc TM Touch Imaging System described above, and normalized to total protein quantified in the sample lane, e.g., the lane in which that protein was electrophoresed, using Bio-Rad proprietary stain-free imaging gel technology and instrumentation with Image Lab™ 6.0.0 software, as described at http://www.bio-rad.com/en-us/applications-technologies/stain-free-imaging-technology?ID=NZ0G1815. This superior method for Western blot normalization distinctly diminishes data variability through improved measurement accuracy and precision (Gilda and Gomes, 2015; Moritz, 2017). Precision plus protein molecular weight dual color standards (prod. no. 161–0374, Bio-Rad) were included in each Western blot analysis.

2.3. LH radioimmunoassay

Plasma LH concentrations were measured by radioimmunoassay, as described [Singh and Briski (Singh and Briski, 2004)].

2.4. Statistical Analyses

Mean normalized DβH, GCK, SUR-1, ERα, ERβ, and GPER mRNA values for A2 noradrenergic neurons identified as (1) cytoplasmic retrobead epifluorescence-positive, cytoplasmic TH-ir-positive, and nuclear GKRP-ir-positive or (2) cytoplasmic retrobead epifluorescence-positive, cytoplasmic TH-ir-positive, and nuclear GKRP-ir-negative; normalized rPO GnRH-I protein O.D. measures; and plasma LH concentrations were analyzed by two-way analysis of variance and Student-Newman-Keuls *post-hoc* test, using GraphPad Prism (Volume 8).

Differences of $p < 0.05$ established by *post-hoc* analysis between group means were considered significant. In each figure, statistical differences between specific pairs of treatment groups are indicated by the following symbols: *$p < 0.05$; **$p < 0.01$; ***$p < 0.001$.

3. Results

Fig. 1 depicts representative A2 noradrenergic neurons that exhibit dual cytoplasmic TH-ir-positive immunostaining (Panel I) and Retrobead retrograde tracer epifluorescence (Panel II) in the presence (neurons identified by red or yellow arrow) or absence (neuron depicted in Panel insets; denoted by green arrow) of nuclear GKRP-ir (Panel III). Mean total numbers of TH-ir-positive A2 neurons counted per animal were 62 +/- 7 and 69 +/- 8 for FF/E-300 and FF/E-30 groups, respectively [$F_{(3,16)}$= 0.42, $p = 0.514$]; these numbers did not differ between FF versus FD groups at either E dosage. Counts of TH-ir-positive neurons projecting to the rPO were 14 +/- 2 (FF/E-300) or 13 +/- 2 (FF/E-30) [$F_{(3,16)}$= 0.13, $p = 0.742$], measures that were unaffected by FD. FF/E-300 animals had 7 +/- 1 TH-ir-/epifluorescence-positive A2 neurons that exhibited nuclear GKRP-ir and 6 +/- 1 TH-ir-/epifluorescence-positive GKRP-ir-negative A2 neurons; these respective means did not vary among the four treatment groups [$F_{(3,16)}$= 1.45, $p = 0.267$; $F_{(3,16)}$= 1.24, $p = 0.315$].

Data in Fig. 2 illustrate patterns of DβH gene expression in GKRP-ir-positive versus GKRP-ir-negative A2 noradrenergic neurons from full-fed (FF) versus food-deprived (FD) groups of OVX female rats implanted with high- (300 ug/mL; E-300) versus low- (30 ug/mL; E-30) dose E. Data indicate that GKRP-ir-positive A2 nerve cell DβH mRNA content was significantly higher in FF/E-300 (solid white bar) versus FF/E-30 (solid gray bar) groups (Fig. 2A). Yet, results in Fig. 2B show that these transcripts were expressed at equivalent levels in GKRP-ir-negative A2 neurons acquired from FF/E-300 or FF/E-30 animals. FD caused a significant decline in GKRP-ir-positive A2 nerve cell DβH gene expression in E-300 rats [FD/E-300 (striped white bar) versus FF/E-300 (solid white bar)], but elevated this mRNA profile in this A2 cell type in E-30 animals [FD/30 (striped gray bar) versus FF/E-30 (solid gray bar)] (Fig. 2A). FD did not alter DβH mRNA levels in GKRP-ir-negative A2 neurons in either E-300 or E-30 animals (Fig. 2B).

Fig. 3 depicts effects of FD on GCK (Fig. 3A and 3B) and SUR-1 (Fig. 3C and 3D) gene expression in GKRP-ir-positive versus -ir-negative A2 neurons from E-300 and E-30 animals. As shown in Fig. 3A, GKRP-ir-positive neurons had significant up-regulated GCK mRNA during E positive-feedback [FF/E-300 (solid white bar) versus FF/E-30 (solid gray bar)], which was abolished by FD. Meanwhile FD stimulated GCK mRNA in FF/E-30 rats. GKRP-ir-negative A2 neurons from E-300 or E30 animals did not exhibit any difference in this gene profile. Both GKRP-ir-positive and -ir-negative A2 nerve cells showed no effect of E positive feedback on SUR-1 mRNA level. FD did not alter SUR-1 transcript level in E-300 animals, but significantly suppressed this gene profile in E-30 rats [FD/E-30 versus (striped gray bar) versus FF/E-30 (solid gray bar)].

Data presented in Fig. 4 portray effects of FD on patterns of A2 noradrenergic neuron ERα (Fig. 4A and 4B) and ERβ (Fig. 4C and 4D) gene expression in E-300 versus E-30 animals. As shown in Fig. 4A, ERα mRNA content was not different between GKRP-ir-positive A2 neurons taken from FF/E-300 versus FF/E-30 animals. Data presented in Fig. 4B show that this GKRP-ir-negative A2 cell transcript profile did not vary between high- versus low-E groups. FD caused significant up-regulation
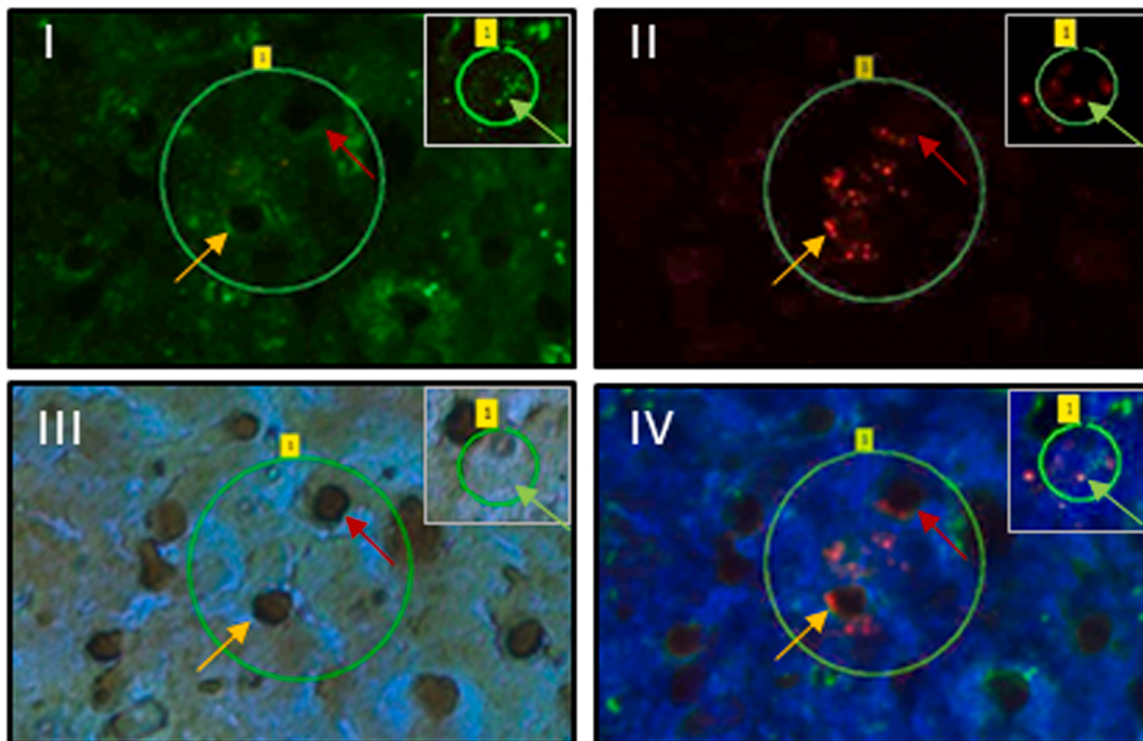

Fig. 1. Identification of Rostral Preoptic Area (rPO)-Projecting A2 Noradrenergic Neurons by Dual Cytoplasmic Retrobead Epifluorescence and Tyrosine Hydroxylase (TH)-Immunoreactivity (-ir) and Their Sub-Categorization According to Presence versus Absence of Nuclear Glucokinase Regulatory Protein (nGKRP) Immunolabeling. Ovariectomized (OVX) rats were implanted with a subcutaneous (*sc*) estradiol (E)-filled silastic capsule [30 ug E/mL (E-30) versus 300 ug E/mL (E-300)], then injected into the rPO with Retrobead retrograde tracer prior to 18 h food deprivation (FD) or uninterrupted feeding (full-fed, i.e., FF controls). Hindbrain A2 neurons were identified *in situ* by tyrosine hydroxylase (TH)-immunoreactivity (-ir) (Panel I); TH-ir-positive cells exhibiting red cytoplasmic tracer epifluorescence (Panel II) were individually laser-catapult-microdissected for single-cell multiplex qPCR following sub-categorization based upon the presence or absence of nGCKR-ir (Panel III). The encircled area in Panels I, II, and III contains two representative cytoplasmic TH-ir- and Retrobead epifluorescence-positive hindbrain A2 neurons (one indicated by a yellow arrow, the other by a red arrow) that exhibit immunostaining for nGKRP-ir. Panel IV presents a merged image of cytoplasmic and nuclear staining patterns. The inset to each Panel, upper right-hand corner, shows an encircled TH-ir- and Retrobead epifluorescence-positive neuron that lacks nGKRP-ir.
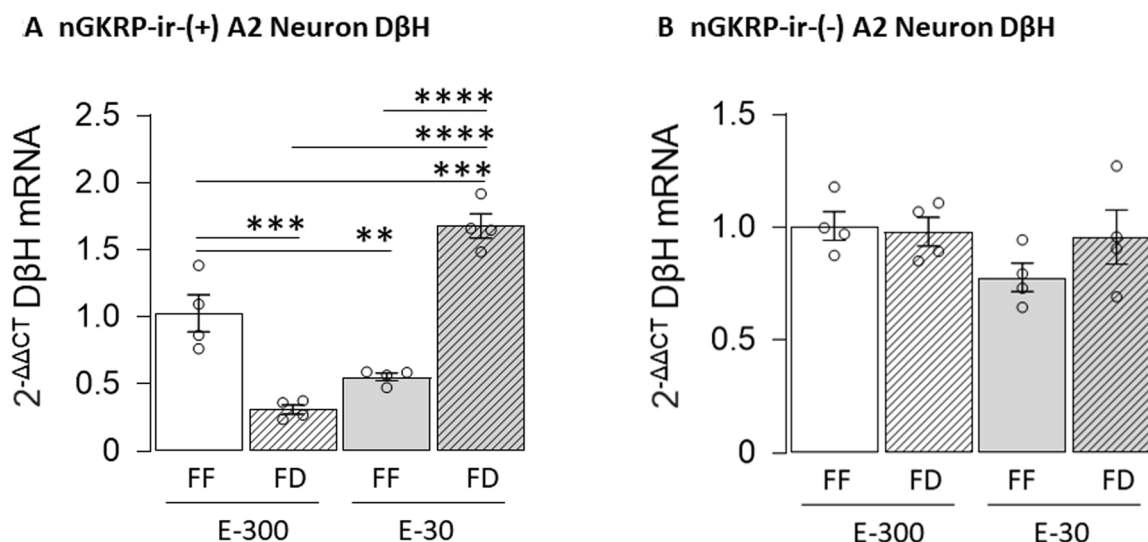
Fig. 2. Effects of Short-Term Food Deprivation (FD) on Dopamine-Beta-Hydroxylase (DβH) and TH Gene Expression in A2 Noradrenergic Neurons Innervating the rPO of Estradiol-Implanted OVX Female Rats. Graphs depict mean normalized DβH mRNA levels +/- S.E.M. measured in cytoplasmic epifluorescence-positive, cytoplasmic TH-ir-positive, nGKRP-ir-positive A2 neurons (Fig. 2A) or cytoplasmic epifluorescence-positive, cytoplasmic TH-ir-positive, nGKRP-ir-negative (Fig. 2B) A2 neurons collected from FF/E-300 (solid white bars; n = 4 nGKRP-ir-positive A2 nerve cells; n = 4 nGKRP-ir-negative A2 neurons; FD/E-300 (striped white bars; n = 4 nGKRP-ir-positive A2 nerve cells; n = 4 nGKRP-ir-negative A2 neurons), FF/E-30 (solid gray bars; n = 4 nGKRP-ir-positive A2 nerve cells; n = 4 nGKRP-ir-negative A2 neurons), or FD/E-30 (striped gray bars; n = 4 nGKRP-ir-positive A2 nerve cells; n = 4 nGKRP-ir-negative A2 neurons) treatment groups. Data were analyzed by two-way ANOVA and Student-Neuman-Keuls *post-hoc* test, using GraphPad Prism (Volume 8) software; statistical results are presented in Supplementary Table 1. *$p < 0.05$; **$p < 0.01$; ***$p < 0.001$; ****$p < 0.0001$.

of ERα gene transcription in FD-30 [FD/E-30 versus FF/E-30], but not FD-300 animals. Fig. 4C shows that ERβ gene expression was equivalent in GKRP-ir-positive A2 neurons from E-300 versus E-30 groups, and resistant to effects by FD. This gene profile was also refractory to either E positive-feedback or FD in GKRP-ir-negative A2 cells (Fig. 4D).

Fig. 5 depicts effects of FD on plasma glucose (Fig. 5A), rPO GnRH-1 protein content (Fig. 5B), and plasma LH concentrations (Fig. 5C) in E-300 and E-30 animals. As shown in Fig. 5A, mean plasma glucose levels were unaffected by FD in either E treatment group. Data in Fig. 5B show that rPO GnRH-1 levels were significantly augmented in E-300 versus E-30 animals, but that this increase was abolished by FD. FD had no impact on tissue GnRH-1 content in E-30 rats. Plasma LH levels were elevated in response to E positive feedback [FF/E-300 versus FF/E-30]. This hormone profile was significantly diminished in FD/E-300 versus FF/E-300 groups. However, FD did not alter circulating LH concentrations in E-30 rats.

4. Discussion

Current data provide unique proof that individual A2 neurons that project to the female rat rPO express classical ER variant and metabolic sensor biomarker genes. These cells exhibit either discriminative (nGKRP-ir-positive A2 neurons) or uniform (nGKRP-ir-negative A2 neurons) DβH transcriptional responses to bimodal E signaling, implicating the former subpopulation in mediating E positive-feedback activation of the reproductive neuroendocrine axis. Interestingly, DβH and GCK mRNAs are sensitive to short-term FD-associated metabolic imbalance only in nGKRP-ir-positive A2 cells; it remains to be determined whether these gene responses are causally related. FD-responsive A2 nerve cells from high- or low-E-dose rats exhibit contrary adjustments in DβH and GCK gene transcripts as these profiles are down-regulated in high-E-dosed rats, yet up-regulated in animals given the low E dosage. These results support the novel notion that FD respectively suppresses or enhances positive- versus negative-feedback – driven NE signaling to the rPO. Correlation of metabolic regulation of DβH and GCK mRNAs with the presence of nGKRP-ir infers that GKRP-mediated control of GCK activity may be required for monitoring of

metabolizable glucose. Evidence here for FD regulation of ERα mRNA content in low-E, but not high-E A2 neurons implicates this ER variant in FD-mediated gene responses during E negative feedback.

Physiological relevance of novel observational data described here includes unanticipated identification of nGKRP as a biomarker for metabolic-sensitive A2 neurons innervating the rostral preoptic area. Importantly, this concept refutes the long-held view that the presence of GCK distinguishes metabolic-sensory neurons from those that do not perform this function, as data here show that GCK mRNA profiles were refractory to food deprivation in A2 nerve cells that lack nGKRP-ir. Current work, moreover, introduces definitive proof that metabolic-sensitive, but not -insensitive A2 neurons function as a common target for hormonal and metabolic inputs, results that suggest that these cells are critical not only for positive-feedback stimulation of the reproductive neuroendocrine axis, but also, paradoxically, for curtailment of this activated state due to metabolic insufficiency.

Study outcomes show that DβH and GCK mRNA profiles in rPO-projecting nGKRP-ir-positive A2 neurons were significantly greater in high-E/FF versus low-E/FF animals. This documentation of E positive-feedback stimulation of DβH gene expression infers that patterns of preoptic NE signaling elicited by this steroid feedback mode emanate, in part, from nGKRP-expressing A2 cells. It is noted that quantitative measures of experimental manipulations of mRNA expression should not be construed as definitive proof of equivalent changes in corresponding gene product protein profiles. Surprisingly, DβH mRNA levels in nGKRP-ir-negative A2 neurons did not differ between high-E/FF versus low-E/FF animals, implying that noradrenergic input to the rPO from these cells may be refractory to E positive-feedback. As ERα and ERβ mRNAs are expressed in each A2 subpopulation, unvarying versus divergent DβH responses to high- and low-E dosing could reflect, in part, differential cellular receptivity to E owing to dissimilar ERα and/or ERβ protein profiles. Observations here of treatment-associated changes in catecholamine biosynthetic enzyme gene expression are qualified by consideration that this experimental parameter constitutes an indirect indicator of potential adjustments in nerve cell synaptic firing and chemical transmission.

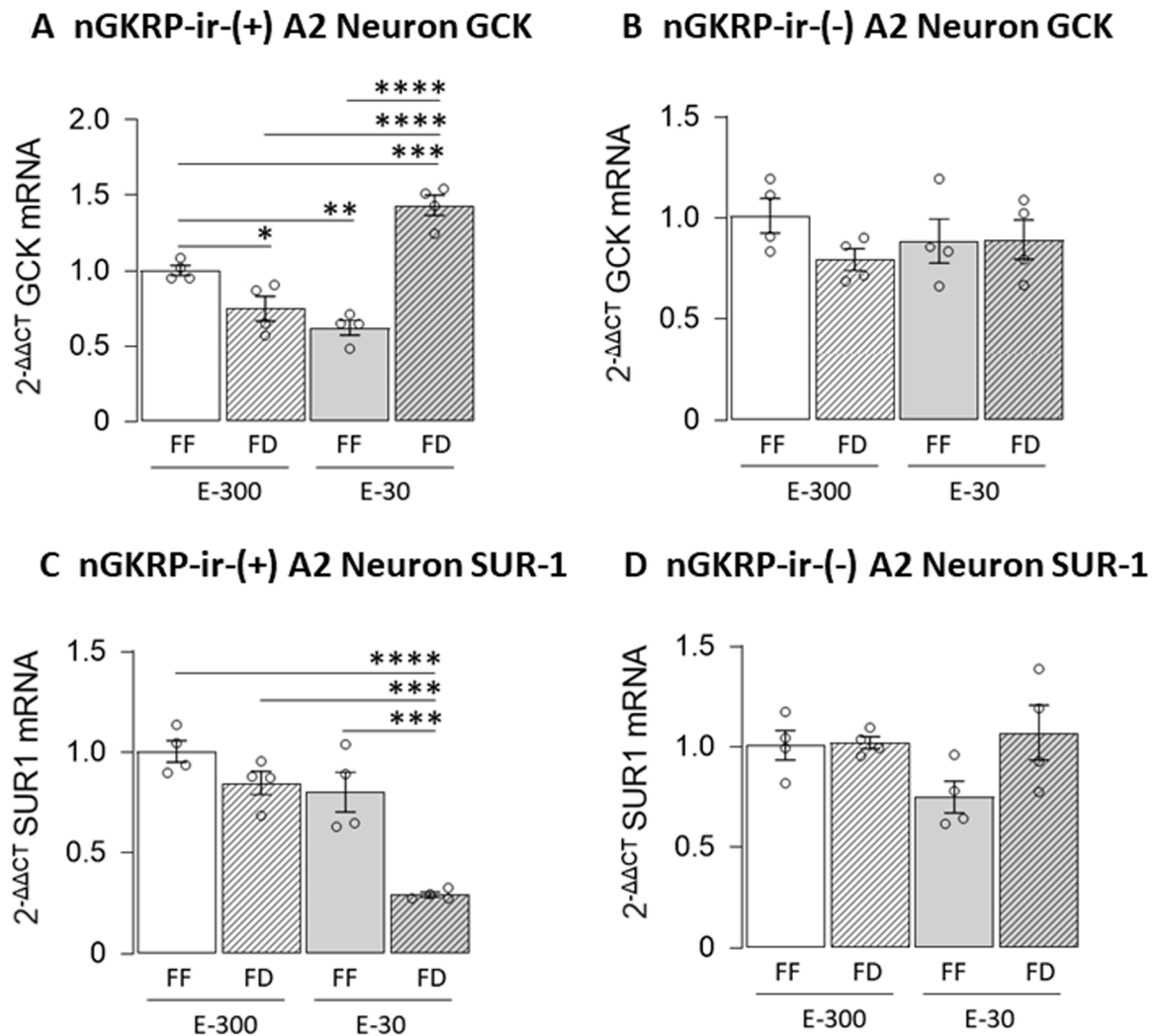The specialized hexokinase GCK catalyzes non-reversible, product-

Fig. 3. Effects of High (E-300) versus Low (E-30) Estradiol Dosing on Glucokinase (GCK) and Sulfonylurea Receptor-1 (SUR-1) mRNA Responses to FD in rPO-Projecting A2 Noradrenergic Neurons. Data show mean normalized GCK or SUR-1 mRNA levels +/- S.E.M. measured in cytoplasmic epifluorescence-positive, cytoplasmic TH-ir-positive, nGKRP-ir-positive A2 neurons (Fig. 3A and 3C) or cytoplasmic epifluorescence-positive, cytoplasmic TH-ir-positive, nGKRP-ir-negative (Figs. 3B and 3D) A2 neurons collected from FF/E-300 (solid white bars; n = 4 nGKRP-ir-positive A2 nerve cells; n = 4 nGKRP-ir-negative A2 neurons), FD/E-300 (striped white bars; n = 4 nGKRP-ir-positive A2 nerve cells; n = 4 nGKRP-ir-negative A2 neurons), FF/E-30 (solid gray bars; n = 4 nGKRP-ir-positive A2 nerve cells; n = 4 nGKRP-ir-negative A2 neurons), or FD/E-30 (striped gray bars; n = 4 nGKRP-ir-positive A2 nerve cells; n = 4 nGKRP-ir-negative A2 neurons) treatment groups. Data were analyzed by two-way ANOVA and Student-Neuman-Keuls *post-hoc* test, using GraphPad Prism (Volume 8) software; statistical results are presented in Supplementary Table 1. *p < 0.05; * *p < 0.01; ***p < 0.001; ****p < 0.0001.

independent phosphorylation of glucose in the initial step of the glycolytic pathway and functions as a glucose sensor (Matschinsky and Wilson, 2019). A novel discovery here is that bimodal E feedback promotes divergent patterns of GCK gene transcription in nGKRP-ir-positive A2 neurons, inferring that glycolytic pathway activity and glucose-sensory functionality in this A2 subtype may vary according to E signal volume. Further work is needed to determine if enhanced GCK gene expression in the presence of E positive-feedback correlates with hormone-induced augmentation of cellular glucose uptake and catabolism via glycolysis, and if so, whether a potential gain in cellular positive energy balance is an impetus for enhanced catecholamine biosynthesis and transmission associated with exposure to high E.

A2 noradrenergic neurons characterized by differential DβH responses to bimodal E feedback show transcriptional reactivity of this gene profile to FD, yet A2 neurons that exhibit uniform DβH expression during E positive- versus negative-feedback had no change in this transcript profile during FD. Ongoing work seeks to address if and how A2 sensitivity to these hormonal and metabolic cues may be coordinately regulated. Intriguingly, data here show that E feedback mode

determines the direction of FD-associated change on DβH mRNA levels, as transcription was increased or decreased in nGKRP-ir-positive A2 neurons obtained from low-E/FD versus high-E/FD animals, respectively. Thus, FD evidently augments NE signaling to the rPO when E negative feedback is in effect, yet attenuates E positive-feedback - stimulated noradrenergic transmission to this structure. Estrogenic and metabolic cues to reproductive neuroendocrine function are contradictory when E positive-feedback is operative, as these signals respectively stimulate or suppress axis activity. Data here identify nGKRP-ir-positive A2 neurons as a common substrate for steroidal and metabolic regulation of NE signaling to the rPO, and infer that metabolic imbalance may act as a brake on steroidal activation of the GnRH-LH axis by repressing E-stimulated noradrenergic transmission. It would be informative to understand mechanisms responsible for bi-directional E concentration-dependent effects of FD on DβH transcription in A2 nerve cells. It is relevant to consider if, during one or both modes of E feedback, FD may directly regulate DβH gene transcriptional responses to E input and/or control ER variant protein expression to modulate ER signal volume governing DβH mRNA production. Current evidence that FD reverses E
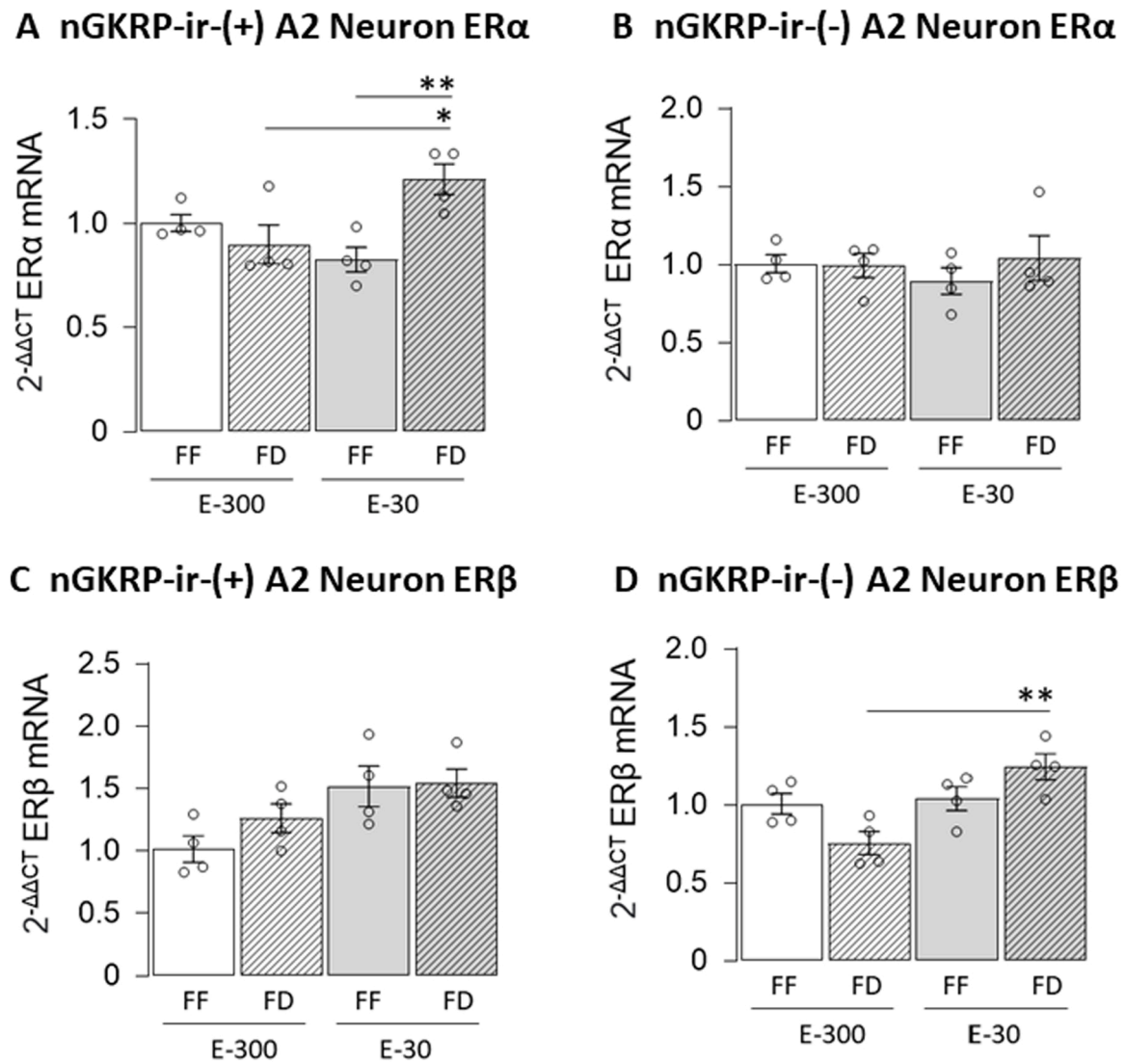
Fig. 4. Effects of FD on Estrogen Receptor-Alpha (ERα) and Estrogen Receptor-Beta (ERβ) Gene Expression in rPO-Projecting A2 Noradrenergic Neurons from High E- versus Low E-Treated OVX Rats. Results depict show mean normalized ERα or ERβ mRNA levels +/- S.E.M. in cytoplasmic epifluorescence-positive, cytoplasmic TH-ir-positive, nGKRP-ir-positive A2 neurons (Fig. 4A and 4 C) or cytoplasmic epifluorescence-positive, cytoplasmic TH-ir-positive, nGKRP-ir-negative (Figs. 4B and 4D) A2 neurons collected from FF/E-300 (solid white bars; n = 4 nGKRP-ir-positive A2 nerve cells; n = 4 nGKRP-ir-negative A2 neurons), FD/E-300 (striped white bars; n = 4 nGKRP-ir-positive A2 nerve cells; n = 4 nGKRP-ir-negative A2 neurons), FF/E-30 (solid gray bars; n = 4 nGKRP-ir-positive A2 nerve cells; n = 4 nGKRP-ir-negative A2 neurons), or FD/E-30 (striped gray bars; n = 4 nGKRP-ir-positive A2 nerve cells; n = 4 nGKRP-ir-negative A2 neurons) treatment groups. Data were analyzed by two-way ANOVA and Student-Neuman-Keuls *post-hoc* test, using GraphPad Prism (Volume 8) software; statistical results are presented in Supplementary Table 1. *p < 0.05; **p < 0.01; ***p < 0.001; ****p < 0.0001.

positive-feedback augmentation of rPO GnRH-1 protein expression and circulating LH levels affirms prior documentation that this metabolic stress represses reproductive neuroendocrine function (Shakya et al., 2018).

Electrophysiological mapping of the DVC showed that 'glucose-excited (GE)' and 'glucose-inhibited (GI)' neurons are confined primarily to the A2 cell group area (Mizuno and Oomura, 1984), where both phenotypes were ascribed to catecholaminergic neurons (Yettefti et al., 1997). Recent studies involving male rats suggest that A2 neurons may likely signal varying intensities or nature of metabolic imbalance in part by reducing or amplifying NE signal strength (Alshamrani et al., 2020). A critical question concerns whether distinct subsets of A2 neurons operate exclusively as GE or GI, or if individual A2 cells are capable of bi-directional signaling depending upon extent/type of metabolic instability. Indeed, E positive-feedback stimulation of DβH gene expression in nGKRP-ir-positive cells may reflect GE metabolic signaling of positive energy balance by these cells. Present data infer that

nGRKP-ir-positive A2 neurons may notify metabolic imbalance in the form of enhanced GI or diminished GE transmission in the presence of E negative- versus positive-feedback, respectively. FD increased ERα mRNA levels in nGKRP-ir-positive neurons from low-E, but not high-E rats, implying that this ER variant may play a role in differential transcriptional responses elicited by E bimodal feedback. As this gene profile was refractory to FD in nGKRP-ir-negative A2 neurons from low-E rats, GKRP regulation of GCK is evidently required for metabolic regulation of ERα gene expression during FD.

FD was observed here to amplify or suppress GCK gene expression in nGKRP-ir-positive A2 nerve cells in low-E versus high-E rats. It is unclear if the direction of this gene response is controlled by E independent of cellular metabolic status. Alternatively, in light of evidence for parallel FD effects on DβH and GCK transcription in each E treatment group, up- or down-regulated GCK expression may reflect adaptation of energy production pathways to FD-induced increases or reductions in DβH expression and corresponding NE synthesis and signaling. In nGKRP-ir-
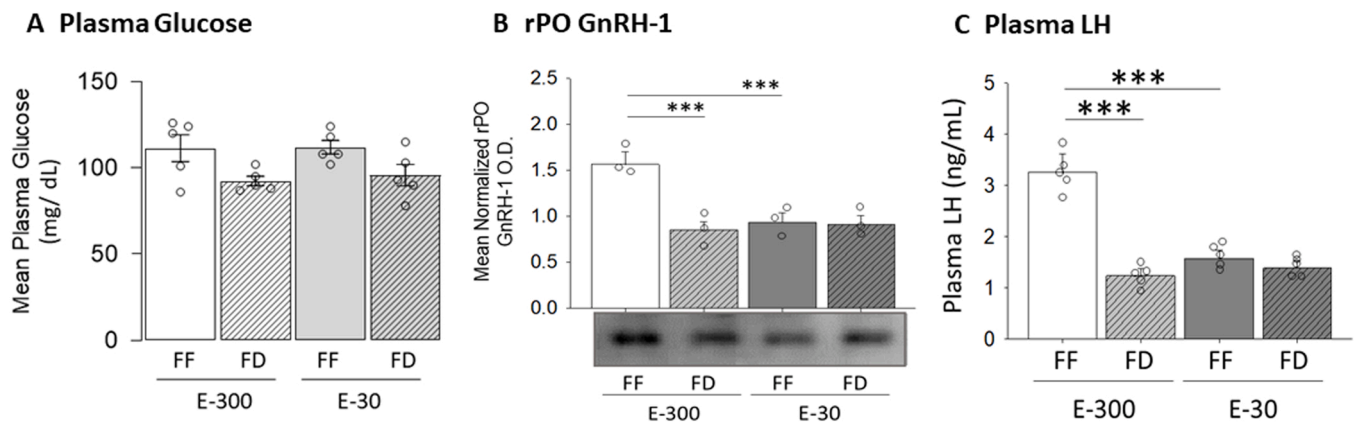
Fig. 5. Effects of FD on Plasma Glucose Levels, rPO Gonadotropin-Releasing Hormone-1 (GnRH-1) Content, and Plasma Luteinizing Hormone (LH) Concentrations in High E- versus Low E-Treated OVX Rats. Data illustrate FD effects on mean plasma glucose levels (Fig. 5 A; n = 5/group), mean normalized rPO GnRH-1 tissue content (Fig. 5B; n = 3 lysate pools/group) or mean plasma LH levels (Fig. 5 C; n = 5 group) +/- S.E.M. for the following treatment groups: FF/E-300 (solid white bars), FD/E-300 (striped white bars), FF/E-30 (solid gray bars), or FD/E-30 (striped gray bars) treatment groups. Data were analyzed by two-way ANOVA and Student-Neuman-Keuls *post-hoc* test, using GraphPad Prism (Volume 8) software; statistical results are presented in Supplementary Table 1. *p < 0.05; * *p < 0.01; * **p < 0.001; * ** *p < 0.0001.

positive A2 neurons from low-E/FD rats, it is not known if cell glucose uptake is altered to match a likely increase in energy demand; unfortunately, this issue remains unresolved as current analytical tools lack requisite sensitivity for single-cell glucose measurements *in situ*. There is a need to elucidate the sensory role GCK may play, if any, in detection of FD-associated A2 nerve cell metabolic instability and regulation of cellular function, including NE signaling. K_{ATP} is an energy sensor that augments synaptic firing by membrane depolarization, and is associated with hypothalamic GE metabolic-sensory neuron function (Cotero and Routh, 2009; Gonzàlez et al., 2009). Current data indicate that the K_{ATP} channel subunit SUR-1 is transcribed at comparable levels in nGKRP-ir-positive A2 neurons from high- versus low-E treatment groups, but that this gene profile is only responsive to FD in the presence of low E. Observations of down-regulated SUR-1 gene expression in low-E/FD rats may reflect a shift from GE to GI nerve cell metabolic sensory machinery. It should be noted that GE neurons are reported to also utilize K_{ATP}-independent mechanisms to translate glucose availability into synaptic firing (Fioramonti et al., 2004; Burdakov et al., 2005). Still at issue is the question of the role of AMPK in FD effects on DβH gene expression during E negative- versus positive-feedback. Ongoing studies seek examine whether A2 nerve cell-specific AMPK gene knockdown will prevent or attenuate gene responses to FD documented here.

GKRP binds to GCK in competition with glucose to regulate GCK enzyme activity and subcellular localization. Falling cellular glucose levels promote GCK-GKRP complexation, resulting in GCK deactivation and sequestration in the nucleus. Studies on the distribution of GKRP within the brain are few (Alvarez et al., 2002; Roncero et al., 2009), and the identity of brain cell types that express this regulatory enzyme is not known. Data here show that a subset of A2 neurons exhibit nuclear immunolabeling for GKRP-ir, and importantly, these, but not nGKRP-ir-negative A2 nerve cells exhibit discriminative DβH and GCK transcriptional responses to bimodal E feedback. Observations that nGKRP-ir is present in A2 neurons from FF and FD animals are consistent with reports that GKRP is primarily localized to the nucleus of cultured hepatocytes at both low and high glucose concentrations (de la Iglesia et al., 1999). It would be of immense benefit to discover how GKRP control of GCK activity enables A2 nerve cell sensitivity to estrogenic and metabolic regulatory cues. It can be speculated that GKRP-associated deactivation of unoccupied GCK may generate a sensitive readout of cellular metabolizable glucose by mechanisms that involve close coupling of active cytoplasmic GCK and glucose concentrations and/or by as-yet-unknown regulatory effects on cytoplasmic

GCK activity.

In the absence of net change in plasma glucose levels despite curtailment of feeding for 18 h, the identity of regulatory cues that affect catecholamine enzyme and metabolic-sensory biomarker gene expression in nGKRP-ir-positive, but not nGKRP-ir-negative A2 neurons can only be speculated at present. There is an obvious need for further research to determine whether FD imposed over the time frame employed here elicits peripheral signals emanating from the gastrointestinal tract (i.e. hepatic portal vein glucose sensors; hepatic glycogenolysis) or adipose tissue (leptin, adiponectin) and/or central cues emanating from astrocyte glycogen energy reserve that are received by A2 neurons, and moreover, how those regulatory inputs may be affected by low versus high estradiol secretory patterns. We are very intrigued that nGKRP-ir-positive neurons are evidently responsive to what may likely be small-scale adjustment(s) in signals that report on metabolic stability, which bolsters the long-held concept that the female reproductive neuroendocrine axis is exquisitely sensitive to metabolic state.

The current study utilized an ovariectomized, estradiol-treated animal model to replicate plasma hormone profiles at levels that correspond to measures associated with metestrus or proestrus stages of the estrous cycle. This approach brings the benefit of normalized circulating estradiol concentrations among subjects, but is impeded by deviation from the normal physiological circumstance of exposure to dynamic day-to-day fluctuations in endogenous steroid secretion over the course of the estrous cycle. Thus, the prospect that constant versus transient exposure to metestrus- and/or proestrus-like plasma estradiol levels may result in discrepant effects of FD on A2 nerve cell gene profiles investigated here cannot be overlooked.

In summary, current studies provide novel evidence that distinct caudal DVC A2 noradrenergic neurons populations exhibit altered versus unaffected transmission to the female rat rPO during FD-associated metabolic imbalance, and that E feedback mode controls the direction of this change in noradrenergic signaling. FD-responsive A2 cells projecting to the rPO display nuclear GKRP-ir, but show divergent adjustments in GCK mRNA expression, i.e. down- (high-E dosage) versus up-regulated (low-E dosage). Outcomes characterize nGKRP-ir-positive A2 neurons as a common substrate for steroidal and metabolic regulation of NE input to the rPO, inferring that metabolic instability may curb E activation of the GnRH-LH axis through repression of E positive-feedback stimulation of noradrenergic transmission. Further studies are needed to determine how bimodal E signal volumes regulate neurotransmitter and metabolic sensor responses to FD in GKRP-expressing rPO-projecting A2 neurons in the presence of GKRP.

CRediT authorship contribution

Alshamrani, Ayed: Investigation, Formal analysis, Data curation, Visualization **Ibrahim, Mostafa M.H.**: Investigation, Formal analysis **Briski, Karen P.**: Conceptualization, Resources, Supervision, Writing – original draft, Writing – review & editing, Project administration, Funding acquisition.

Acknowledgements

Appendix A. Supporting information

Supplementary data associated with this article can be found in the online version at doi:10.1016/j.ibneur.2022.06.001.

References

Agius, L., 2008. Glucokinase and molecular aspects of liver glycogen metabolism. Biochem. J. 414, 1–18. https://doi.org/10.1042/BJ20080595.

Agius, L., 2016. Hormonal and metabolite regulation of hepatic glucokinase. Annu. Rev. Nutr. 36, 389–415. https://doi.org/10.1146/annurev-nutr-071715-051145.

Adler, B.A., Johnson, M.D., Lynch, C.O., Crowley, W.R. Evidence that norepinephrine and epinephrine systems mediate the stimulatory effects of ovarian hormones on luteinizing hormone and luteinizing hormone-releasing hormone.

Alenazi, F.S.H., Ibrahim, B.A., Alhamami, H., Shakya, M., Briski, K.P., 2016. Role of estradiol in intrinsic hindbrain AMPK regulation of hypothalamic AMPK, metabolic neuropeptide, and norepinephrine activity and food intake in the female rat. Neuroscience 314, 35–46.

Alshamrani, A., Bheemanapally, K., Ibrahim, M.M.H., Briski, K.P., 2020. Impact of caudal hindbrain glycogen metabolism on A2 noradrenergic neuron AMPK activation and ventromedial hypothalamic nucleus norepinephrine activity and glucoregulatory neuro-transmitter marker protein expression. Neuropeptides 82, 102055.

Alvarez, E., Roncero, I., Chowen, J.A., Vasquez, P., Blazquez, E., 2002. Evidence that glucokinase regulatory protein is expressed and interacts with glucokinase in rat brain. J. Neurochem. 80, 45–53.

Briski, K.P., Sylvester, P.W., 1998. Effects of the glucose antimetabolite, 2-deoxy-D-glucose (2-DG), on the LH surge and Fos expression by preoptic GnRH neurons in ovariectomized, steroid-primed rats. J. Neuroendocrinol. 10, 769–776.

Briski, K.P., Marshall, E.S., Sylvester, P.W., 2001. Effects of estradiol on glucoprivic transactivation of catecholaminergic neurons in the female rat caudal brainstem. Neuroendocrinology 73, 369–377.

Briski, K.P., Koshy Cherian, A., Genabai, N.K., Vavaiya, K.V., 2009. In situ coexpression of glucose and monocarboxylate transporter mRNAs in metabolic-sensitive dorsal vagal complex catecholaminergic neurons: transcriptional reactivity to insulin-induced hypoglycemia (IIH) and caudal hindbrain glucose or lactate repletion during IIH. Neuroscience 164, 1152–1160.

Briski, K.P., Alenazi, F.S.H., Shakya, M., Sylvester, P.W., 2016. Estradiol regulates hindbrain A2 noradrenergic neuron adenosine 5′-monophosphate-activated protein kinase (AMPK) activation, upstream kinase/phosphatase protein expression, and receptivity to hormone and fuel reporters of short-term food deprivation in the ovariectomized female rat. J. Neurosci. Res. 95, 1427–1437.

Burdakov, D., Luckman, S.M., Verkhratsky, A., 2005. Glucose-sensing neurons of the hypothalamus. Philos. Trans. R. Soc. Lond. B Biol. Sci. 360, 2227–2235. https://doi.org/10.1098/rstb.2005.1763.

Butcher, R.L., Collins, W.E., Fugo, N.W., 1974. Plasma concentrations of LH, FSH, progesterone, and estradiol-17beta throughout the 4-day estrous cycle of the rat. Endocrinology 94, 1704–1708.

Cherian, A., Briski, K.P., 2011. Quantitative RT PCR and immunoblot analyses reveal acclimated A2 noradrenergic neuron substrate fuel transporter, glucokinase, phospho-AMPK, and dopamine-beta-hydroxylase responses to hypoglycemia. J. Neurosci. Res. 89, 1114–1124. https://doi.org/10.1002/jnr.22632.

Cotero, V.E., Routh, V.H., 2009. Insulin blunts the response of glucose-excited neurons in the ventrolateral-ventromedial hypothalamic nucleus to decreased glucose. Am. J. Physiol. Endocrinol. Metab. 296 (5), E1101–E1109. https://doi.org/10.1152/ajpendo.90932.2008.

Demling, J., Fuchs, E., Baumert, M., Wuttke, W., 1985. Preoptic catecholamine, GABA, and glutamate release in ovariectomized and ovariectomized estrogen-primed rats utilizing a push-pull cannula technique. Neuroendocrinology 41, 212–218.

Fioramonti, X., Lorsignol, A., Taupignon, A., Pénicaud, L., 2004. A new ATP-sensitive K+ channel-independent mechanism is involved in glucose-excited neurons of mouse arcuate nucleus. Diabetes 53, 2767–2775. https://doi.org/10.2337/diabetes.53.11.2767.

Genabai, N.K., Vavaiya, K.V., Briski, K.P., 2009. Adaptation of glucokinase gene expression in the rat dorsal vagal complex in a model for recurrent intermediate insulin-induced hypoglycemia: impact of gender. J. Mol. Neurosci. 37, 80–86.

Gilda, J.E., Gomes, A.V., 2015. Western blotting using in-gel protein labeling as a normalization control: stain-free technology. Methods Mol. Biol. 1295, 381–391. https://doi.org/10.1007/978-1-4939-2550-6_27.

Giles, E.D., Jackman, M.R., Johnson, G.C., Schedin, P.J., Houser, J.L., MacLean, P.S., 2010. Effect of the estrous cycle and surgical ovariectomy on energy balance, fuel utilization, and physical activity in lean and obese female rats. Am. J. Physiol. Regul. Integr. Comp. Physiol. 299, R1634–R1642.

Gonzàlez, J.A., Reimann, F., Burdakov, D., 2009. Dissociation between sensing and metabolism of glucose in sugar sensing neurones. J. Physiol. 587, 41–48. https://doi.org/10.1113/jphysiol.2008.163410.

Goodman, R.L., 1978. A quantitative analysis of the physiological role of estradiol and progesterone in the control of tonic and surge secretion of luteinizing hormone in the rat. Endocrinology 102, 142–150. https://doi.org/10.1210/endo-102-1-142.

Ibrahim, B.A., Briski, K.P., 2014. Role of dorsal vagal complex A2 noradrenergic neurons in hindbrain glucoprivic inhibition of the luteinizing hormone surge in the steroid-primed ovariectomized female rat: Effects of 5-thioglucose on A2 functional biomarker and AMPK activity. Neuroscience 269, 199–214.

Ibrahim, B.A., Briski, K.P., 2015. Deferred feeding and body weight responses to short-term interruption of fuel acquisition: impact of estradiol. Horm. Metab. Res. 47, 611–621.

Ibrahim, B.A., Tamrakar, P., Gujar, A.D., Koshy Cherian, A., Briski, K.P., 2013. Caudal fourth ventricular administration of the AMPK activator 5-aminoimizaole-4-car-boxamide-riboside regulates glucose and counterregulatory hormone profiles, dorsal vagal complex metabolosensory neuron function, and hypothalamic Fos expression. J. Neurosci. Res. 91, 1226–1238.

de la Iglesia, N., Veiga-da-Cunha, M., Van Schaftingen, E., Guinovart, J.J., Ferrer, J.C., 1999. Glucokinase regulatory protein is essential for proper subcellular localization of liver glucokinase. FEBS Lett. 456, 332–338. https://doi.org/10.1016/S0014-5793(99)00971-0.

Matschinsky, F., Wilson, D.F., 2019. The central role of glucokinase in glucose homeostasis: a perspective 50 years After demonstrating the presence of the enzyme in Islets of Langerhans. Front. Physiol. 10, 148. https://doi.org/10.3389/fphys.2019.00148.

Mizuno, Y., Oomura, Y., 1984. Glucose responding neurons in the nucleus tractus solitarius of the rat: in vitro study. Brain Res. 307, 109–116.

Mohankumar, P.S., Thyagarajan, S., Quadri, S.K., 1994. Correlations of catecholamine release in the medial preoptic area with proestrous surge. Endocrinology 135, 119–126.

Moritz, C.P., 2017. Tubulin or not tubulin: Heading toward total protein staining as loading control in Western blots. Proteomics 17 (20). https://doi.org/10.1002/pmic.201600189.

Ohkura, S., Tanaka, T., Nagatani, S., Bucholtz, D.C., Tsukamura, H., Maeda, K., Foster, D.L., 2000. Central, but not peripheral, glucose-sensing mechanisms mediate glucoprivic suppression of pulsatile luteinizing hormone secretion in the sheep. Endocrinology 141, 4472–4480.

Oomura, Y., Yoshimatsu, H., 1984. Neural network of glucose monitoring system. J. Auton. Nerv. Syst. 10, 359–372.

Roncero, I., Sanz, C., Alvarez, E., Vázquez, P., Barrio, P.A., Blázquez, E., 2009. Glucokinase and glucokinase regulatory proteins are functionally coexpressed before birth in the rat brain. J. Neuroendocrinol. 21, 973–981. https://doi.org/10.1111/j.1365-2826.2009.01919.x.

Shakya, M., Shrestha, P.K., Briski, K.P., 2018. Hindbrain 5′-monophosphate-activated protein kinase mediates short-term food deprivation inhibition of the gonadotropin-releasing hormone-luteinizing hormone axis: role of nitric oxide. Neuroscience 383, 46–59. https://doi.org/10.1016/j.neuroscience.2018.04.040.

Singh, S.R., Briski, K.P., 2004. Septopreoptic mu opioid receptor mediation of hindbrain glucoprivic inhibition of reproductive neuroendocrine function in the female rat. Endocrinology 145, 5322–5331.

Sternisha, S.M., Miller, B.G., 2019. Molecular and cellular regulation of human glucokinase. Arch. Biochem. Biophys. 663, 199–213. https://doi.org/10.1016/j.abb.2019.01.011.

Szawka, R.E., Poletini, M.O., Leite, C.M., Bernuci, M.P., Kalil, B.K., Mendonca, L.B.D., Carolino, R.O.G., Helena, C.V.V., Bertram, R., Franci, C.R., Anselmo-Franci, J.A., 2013. Release of norepinephrine in the preoptic area activates anteroventral periventricular nucleus neurons and stimulates the surge of luteinizing hormone. Endocrinology 154, 363–374.

Tamrakar, P., Ibrahim, B.A., Gujar, A.K., Briski, K.P., 2015. Estrogen regulates energy metabolic pathway and upstream AMPK kinase and phosphatase enzyme expression in dorsal vagal complex metabolo-sensory neurons during glucostasis and hypoglycemia. J. Neurosci. Res. 93, 321–332.

Vavaiya, K.V., Briski, K.P., 2008. Effects of caudal hindbrain lactate infusion on insulin-induced hypoglycemia and neuronal substrate transporter glucokinase and sulfonylurea receptor-1 gene expression in the ovariectomized female rat dorsal vagal complex: impact of estradiol. J. Neurosci. Res. 86, 694–701. https://doi.org/10.1002/jnr.21530.

Wade, G.N., Jones, J.E., 2004. Neuroendocrinology of nutritional infertility. Am. J. Physiol. 287, R1227–R1296.

Wise, P.M., Rance, N., Barraclough, C.A., 1981. Effects of estradiol and progesterone on catecholamine turnover rates in discrete hypothalamic regions in ovariectomized rats. Endocrinology 108, 2186–2193.

Yettefti, K., Orsini, J.C., Perrin, J., 1997. Characteristics of glycemia-sensitive neurons in the nucleus tractus solitarii: possible involvement in nutritional regulation. Physiol. Behav. 61, 93–100.